



**HAL**  
open science

# Remote Sensing of Liquid Water and Ice Cloud Optical Thickness and Effective Radius in the Arctic: Application of Airborne Multispectral MAS Data

M. D. King, S. Platnick, Ping Yang, G. T. Arnold, Mark A. Gray, Jérôme Riédi, S. A. Ackerman, K. N. Liou

► **To cite this version:**

M. D. King, S. Platnick, Ping Yang, G. T. Arnold, Mark A. Gray, et al.. Remote Sensing of Liquid Water and Ice Cloud Optical Thickness and Effective Radius in the Arctic: Application of Airborne Multispectral MAS Data. *Journal of Atmospheric and Oceanic Technology*, 2004, 21 (6), pp.857-875. 10.1175/1520-0426(2004)021%3C0857:RSOLWA%3E2.0.CO;2 . hal-00821793

**HAL Id: hal-00821793**

**<https://hal.science/hal-00821793>**

Submitted on 10 Feb 2021

**HAL** is a multi-disciplinary open access archive for the deposit and dissemination of scientific research documents, whether they are published or not. The documents may come from teaching and research institutions in France or abroad, or from public or private research centers.

L'archive ouverte pluridisciplinaire **HAL**, est destinée au dépôt et à la diffusion de documents scientifiques de niveau recherche, publiés ou non, émanant des établissements d'enseignement et de recherche français ou étrangers, des laboratoires publics ou privés.

## Remote Sensing of Liquid Water and Ice Cloud Optical Thickness and Effective Radius in the Arctic: Application of Airborne Multispectral MAS Data

MICHAEL D. KING,\* STEVEN PLATNICK,+ PING YANG,# G. THOMAS ARNOLD,@ MARK A. GRAY,@  
JÉRÔME C. RIEDI,& STEVEN A. ACKERMAN,\*\* AND KUO-NAN LIOU++

\*Earth Sciences Directorate, NASA Goddard Space Flight Center, Greenbelt, Maryland

+Laboratory for Atmospheres, NASA Goddard Space Flight Center, Greenbelt, Maryland

#Department of Atmospheric Sciences, Texas A&M University, College Station, Texas

@L3 Communications, Government Services, Inc., Landover, Maryland

&Laboratoire d'Optique Atmosphérique, Université des Sciences et Technologies de Lille, Villeneuve d'Ascq, France

\*\*Department of Atmospheric and Oceanic Sciences, University of Wisconsin—Madison, Madison, Wisconsin

++Department of Atmospheric Sciences, University of California, Los Angeles, Los Angeles, California.

(Manuscript received 7 October 2003, in final form 18 November 2003)

### ABSTRACT

A multispectral scanning spectrometer was used to obtain measurements of the bidirectional reflectance and brightness temperature of clouds, sea ice, snow, and tundra surfaces at 50 discrete wavelengths between 0.47 and 14.0  $\mu\text{m}$ . These observations were obtained from the NASA ER-2 aircraft as part of the First ISCCP (International Satellite Cloud Climatology Project) Regional Experiment (FIRE) Arctic Clouds Experiment, conducted over a 1600 km  $\times$  500 km region of the north slope of Alaska and surrounding Beaufort and Chukchi Seas between 18 May and 6 June 1998. Multispectral images in eight distinct bands of the Moderate Resolution Imaging Spectroradiometer (MODIS) Airborne Simulator (MAS) were used to derive a confidence in clear sky (or alternatively the probability of cloud) over five different ecosystems. Based on the results of individual tests run as part of this cloud mask, an algorithm was developed to estimate the phase of the clouds (liquid water, ice, or undetermined phase). Finally, the cloud optical thickness and effective radius were derived for both water and ice clouds that were detected during one flight line on 4 June.

This analysis shows that the cloud mask developed for operational use on MODIS, and tested using MAS data in Alaska, is quite capable of distinguishing clouds from bright sea ice surfaces during daytime conditions in the high Arctic. Results of individual tests, however, make it difficult to distinguish ice clouds over snow and sea ice surfaces, so additional tests were added to enhance the confidence in the thermodynamic phase of clouds over the Chukchi Sea. The cloud optical thickness and effective radius retrievals used three distinct bands of the MAS, with a recently developed 1.62- and 2.13- $\mu\text{m}$ -band algorithm being used quite successfully over snow and sea ice surfaces. These results are contrasted with a MODIS-based algorithm that relies on spectral reflectance at 0.87 and 2.13  $\mu\text{m}$ .

### 1. Introduction

A knowledge of cloud radiative properties and their variation in space and time is especially crucial to the understanding of the radiative forcing of climate. High quality multispectral imagery acquired from high-altitude aircraft or satellite platforms is the most efficient and reliable means of fulfilling these observational requirements. Between 18 May and 6 June 1998, the National Aeronautics and Space Administration (NASA) ER-2 high-altitude research aircraft conducted 11 research flights over the north slope of Alaska and the surrounding Beaufort and Chukchi Seas as part of the First ISCCP (International Satellite Cloud Climatology

Project) Regional Experiment—Arctic Clouds Experiment (FIRE ACE). The NASA ER-2 aircraft was equipped with seven sensors, among which the Moderate Resolution Imaging Spectroradiometer (MODIS) Airborne Simulator (MAS; King et al. 1996) was designed to obtain measurements that simulate those obtained from MODIS, a 36-band spectroradiometer launched aboard the Earth Observing System (EOS) *Terra* (King and Herring 2000) and *Aqua* (Parkinson 2003) spacecraft.

The strategy for FIRE ACE included spaceborne remote sensing (polar-orbiting satellites), high-altitude remote sensing (NASA ER-2 at  $\sim 20$  km), lower-altitude remote sensing and in situ measurements [University of Washington CV-580, National Center for Atmospheric Research (NCAR) C-130Q, and Canada's National Research Council Convair 580 (NRC CV-580) aircraft], ground-based measurements (radiation, clouds, meteo-

Corresponding author address: Dr. Michael D. King, NASA Goddard Space Flight Center, Code 900, Greenbelt, MD 20771.  
E-mail: michael.d.king@nasa.gov

































likely a multilayer cloud with ice clouds overlaying a lower-level Arctic stratus or possibly altostratus layer. As the upper-layer cloud was the dominant feature identified in the multispectral imagery, it is this processing path that was used to estimate cloud optical properties in all subsequent analysis. As described by Shupe et al. (2001) from 1 yr of ground-based radar observations of Arctic clouds from the SHEBA ice station, it is uncommon for Arctic clouds to be single-level water or ice clouds, with either multilayer or mixed-phase clouds occurring some 58.2% of the time during June. The northern portion of this flight track appears to be composed of multilayer clouds, which we will subsequently analyze using the dominant ice cloud libraries characteristic of the uppermost cloud layer (see below).

### b. Cloud optical and microphysical properties

Having identified the corresponding scene as liquid water or ice cloud, we performed cloud optical property retrievals as described in section 3d. Figure 12 shows retrievals of cloud optical thickness and effective radius derived using the retrieval algorithms illustrated in Figs. 7 and 8 for the solar and viewing geometries appropriate to this scene, where the left-hand pair of figures corresponds to the 0.87- and 2.13- $\mu\text{m}$  algorithm and the right-hand pair of figures to the 1.62- and 2.13- $\mu\text{m}$  algorithm. The data points superimposed in Figs. 7 and 8 correspond to southern and northern portions of the flight line that were identified as containing liquid water or ice clouds in Fig. 11. As expected, the effective radius retrievals yield rather similar results between the two algorithms, with the ice cloud particles being quite small in the Arctic region, and where the smallest sizes generally occur for the optically thickest ice clouds in this scene. The failure of the 0.87- and 2.13- $\mu\text{m}$  retrieval in the optically thin northwest portion of this scene occurs because the measured reflection function at 0.87  $\mu\text{m}$  is less than the theoretical calculations allow when  $A_g(0.87 \mu\text{m}) = 0.6$ . This is no doubt the consequences of leads and breaks in the sea ice in this region such that the actual underlying surface albedo is much less than 0.6. This only serves to emphasize the difficulty of using the traditional wavelengths to derive cloud optical thickness and effective radius over a spatially nonuniform sea ice (or snow) surface.

The cloud optical thickness in the traditional 0.87- and 2.13- $\mu\text{m}$  algorithm is especially sensitive to assumptions on the underlying surface albedo, as expected from the computations presented in Fig. 7. King (1987) demonstrates that for optically thick clouds for which asymptotic theory applies ( $\tau_c \geq 9$ ), the derived optical thickness depends explicitly on  $A_g$  such that uncertainties in surface albedo cause a *systematic offset* in the derived optical thickness by an amount given by  $4A_g/3(1-g)(1-A_g)$ , where  $g$  is the asymmetry factor, defined as the mean cosine of the scattering angle obtained by integrating over the complete scattering phase

function ( $\sim 0.85$  for water clouds). This offset is such that the retrieved optical thickness retrieval for  $A_g = 0.5$  (0.7) would be 4.44 *greater* (7.41 *smaller*) than that for  $A_g = 0.6$ . However, as the surface albedo increases to 0.7 and beyond, an increasingly large number of pixels fail the cloud retrieval algorithm because the measured reflectance at 0.87  $\mu\text{m}$  is less than the smallest values expected from theoretical calculations. As a consequence of the uncertainties and variability in the underlying surface albedo of snow and sea ice surfaces at visible wavelengths, the Platnick et al. (2001) algorithm that combines two shortwave infrared bands (1.62 and 2.13  $\mu\text{m}$ ) is especially attractive for cloud optical property retrievals for water clouds. This technique is less sensitive to cloud optical properties of ice clouds due to the strong absorption characteristics of sea ice and ice particles, but both algorithms yield rather similar results for effective radius, even for ice clouds.

A numerical comparison of the two cloud retrieval algorithms can best be seen by examining histograms of retrieved cloud optical properties. Figure 13a shows comparisons of the marginal probability density function of cloud optical thickness for all liquid water clouds in this scene, with Fig. 13b showing the corresponding probability density of effective radius. Figures 13c and 13d show corresponding probability density functions for all ice clouds in this scene, where we have used the same abscissa scale as in Figs. 13a and 13b. Note that a high optical thickness mode ( $\tau_c \geq 100$ ) is not shown on this scale. Though biases clearly exist in the cloud optical thickness retrieval, the effective radius is retrieved quite consistently in both cases. Based on this analysis as well as other retrievals using MAS data in the Arctic (not shown), the 1.62- and 2.13- $\mu\text{m}$  algorithm first described by Platnick et al. (2001) would appear to be a promising algorithm for routine cloud optical property retrievals over snow and sea ice surfaces during the daytime. This algorithm will soon be adapted to MODIS retrievals over these ecosystems for *Terra* data, though the 1.64- $\mu\text{m}$  band on *Aqua*/MODIS is not reliable.

## 5. Summary and conclusions

High-resolution images of the spectral reflection function and thermal emission of the earth-atmosphere system were obtained with the MODIS Airborne Simulator (MAS) operated from the NASA ER-2 aircraft during the intensive field component of the FIRE ACE experiment, conducted over the Beaufort and Chukchi Seas of the Arctic Ocean between 18 May and 6 June 1998. Multispectral images of the reflectance and brightness temperature at 10 wavelengths between 0.66 and 13.98  $\mu\text{m}$  were used to derive the probability of clear sky (or cloud), cloud thermodynamic phase, and the optical thickness and effective radius of liquid water and ice clouds over sea ice in the high Arctic during summer. We compared two separate algorithms for determining

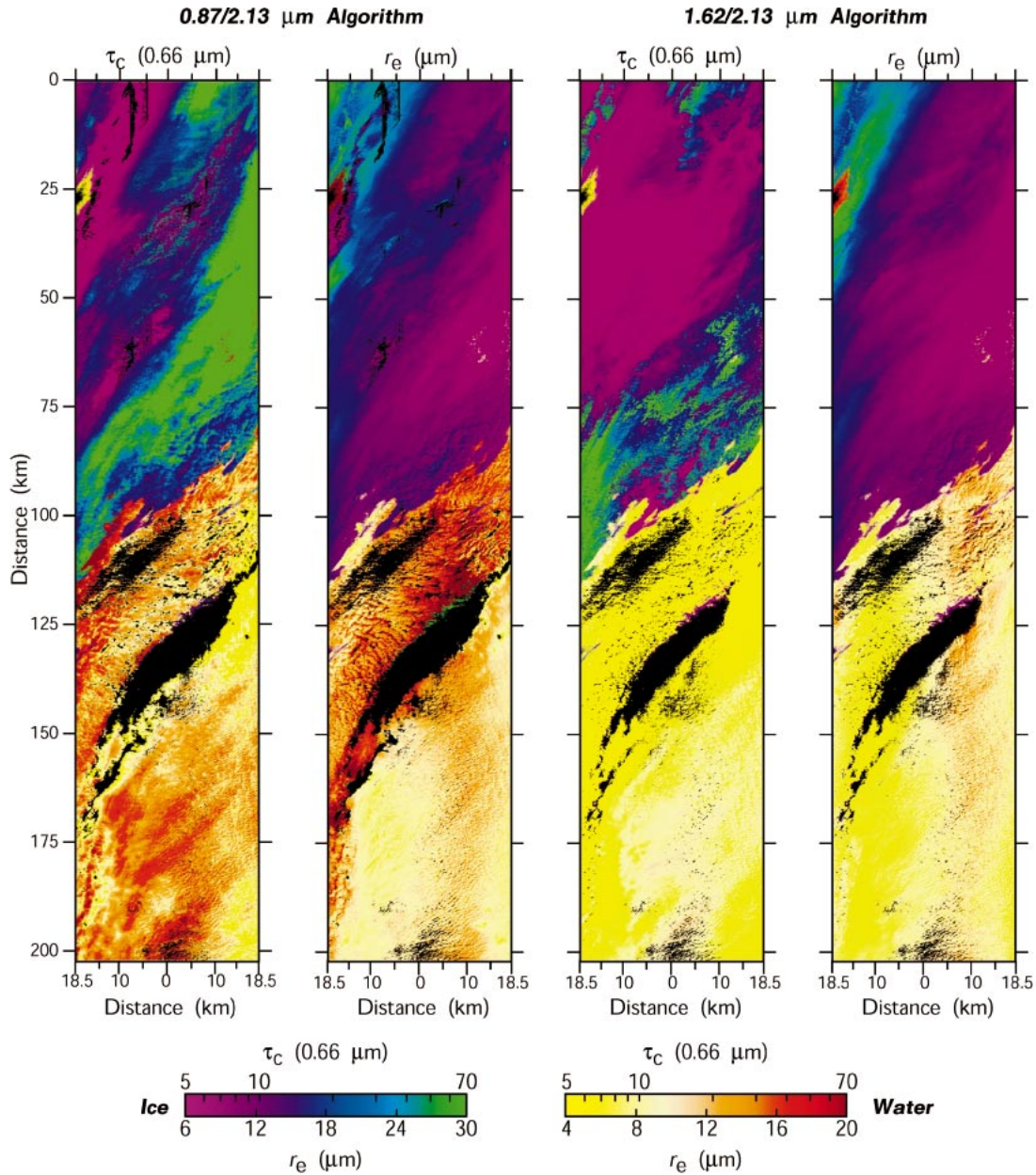


FIG. 12. Cloud optical thickness and effective radius derived from the MAS images on 4 Jun 1998. The pair of images on the left corresponds to the 0.87- and 2.13- $\mu\text{m}$  algorithm, and the pair of images on the right corresponds to the same scene analyzed using the 1.62- and 2.13- $\mu\text{m}$  algorithm. In all cases, we have used a split color bar to designate those pixels analyzed using the liquid water and ice cloud processing path.

the cloud optical thickness and effective radius: one closely aligned to the version run operationally to process MODIS data on the *Terra* and *Aqua* spacecraft, and the other a more recent algorithm that uses the 1.62- and 2.13- $\mu\text{m}$ -band combination.

The 1.62- and 2.13- $\mu\text{m}$  algorithm is more robust at determining the cloud optical thickness and effective radius for water clouds over snow and sea ice surfaces, due primarily to the fact that both snow and sea ice have very low surface reflectance at these wavelengths. As

a consequence, liquid water clouds provide a relatively strong reflectance contrast to the dark underlying surface. This algorithm is less reliable for ice clouds due to the strong absorption by ice particles in both of these bands.

In this paper we also describe the thermodynamic phase algorithm that is nearly identical to that implemented in the global processing of MODIS data from the *Terra* and *Aqua* spacecraft. Both in MAS processing during FIRE ACE and in global processing of MODIS



